Energy Proceedings
Vol 33, 2023
ISSN 2004-2965

Ductile fracture arrest of CO_2 pipelines applied to CCUS technology

Bing Chen, Wenjiao Qi*, Menglin Xu, Sanping Zhou
School of Mechanical Engineering, Xi'an Shiyou University, 710065, Xi'an, Shaanxi, China
(*Wenjiao Qi: wenjiaoqi@xsyu.edu.cn)

ABSTRACT

CO_2 pipeline transportation is the most economical and efficient way to realize CCUS (Carbon Capture, Utilization and Storage) technology, but there is a risk of ductile fracture during its operation due to engineering problems such as pipeline defects, fatigue and corrosion. In this study, a modified Battelle Two-Curve Model and a crack arrest performance evaluation model based on the crack arrest efficiency were established for the pipeline overall reinforcement structure and coaxial crack arrestor, respectively, and the models were verified experimentally to be reliable. Based on the supercritical CO_2 pipeline transportation scheme designed for Yanchang Oilfield with storage capability of 4 million t/a, the crack arrest performance of five pipelines was evaluated. For the non-crackable pipelines, the pipeline overall reinforcement and the coaxial crack arrestor are applied, based on the crack arrest requirement and engineering economy, respectively. This study provides references and suggestions for the design and safe operation of supercritical CO_2 pipelines containing impurities in the future.

Keywords: CCUS; CO_2 pipeline; ductile fracture; arrest control; crack arrestors

1. INTRODUCTION

CO_2 pipeline transportation is a key link in the realization of CCUS technology [1]. However, due to the high pressure of supercritical CO_2 pipeline transportation and the engineering problems such as fatigue and corrosion during the operation of the pipelines, the initial cracks generate. Further affected by the internal pipe pressure, the initial cracks propagate and lead to ductile fracture of the pipelines, seriously affecting safety[2].

Once crack occurs in the pipeline, the medium in the pipeline flows to the crack area, accompanied by the gas expansion phenomenon, results in a decrease in pressure, and thus a decompression wave pressure platform generates, during which period the cracks propagate rapidly. In addition, the medium in the pipe still puts pressure on the cracked pipe wall, eventually leading to the ductile fracture of the cracked pipeline.

Although some CO_2 pipelines are designed to meet the requirements of crack arrest, the performance of the pipelines decreases in the operation process, which may lead to crack propagation at a relatively stable speed[3]. Therefore, in the design of CO_2 pipeline, considering whether the crack can stop propagation after spreading a limited distance without causing the final failure of the pipeline, it is necessary to consider that it should have sufficient ability to prevent ductile fracture propagation. Therefore, different types of crack arrestors can be used to increase the crack arrest toughness, prevent the crack ductile propagation[4].

Cosham[5] conducted three full-scale burst tests, and take the fracture length, CO_2 concentration and initial conditions as research variables. The results show that the Battelle Two-Curve Model (BTCM) cannot be applied to the CO_2 pipelines, same results are also concluded in the full-scale test by Linton[6]. The test results provide a theoretical basis for the modification of BTCM. Therefore, it is necessary to conduct research on the prediction model of ductile fracture arrest of CO_2 pipeline.

Fonzo[7] used the simulation software PICPRO to establish a coaxial crack arrestor with X120 pipeline steel, and optimized its structure. Although the crack arrestors can show good crack arrest performance by reasonable design, it has not been widely used in practical engineering, so it is urgent to develop the crack arrestors suitable for CO_2 pipelines.

Therefore, this research on crack arrest control of ductile fracture of supercritical CO_2 pipeline was carried out to establish a performance evaluation model for crack arrestors that can be directly applied to engineering design. This provides theoretical guidance for the design of crack arrestors to ensure the safe operation of CO_2 transport pipeline.

This is a paper for International CCUS Conference 2023 (ICCUSC2023), April 14-15, 2023, Beijing, China.

2. CRACK ARREST CONTROL THEORY OF SUPERCRITICAL CO_2 PIPELINE

2.1 Pipeline crack arrest criteria

As the theoretical basis for ductile fracture control of pipelines, crack arrest criterion can be divided into energy criterion and velocity criterion based on dynamic fracture mechanics theory. BTCM is the main method of the velocity criterion[8], as shown in Fig. 1.

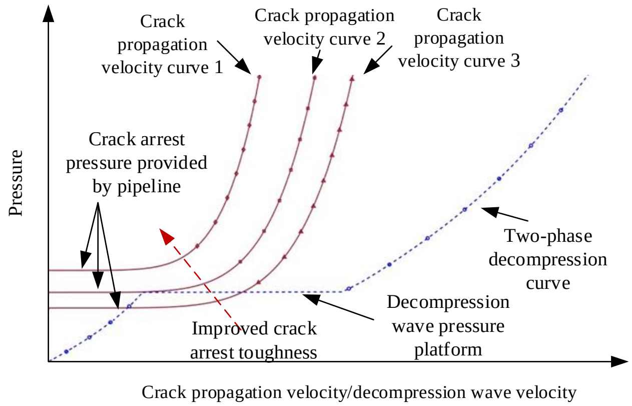

Fig. 1. Battelle Two-Curve Method[8]

According to the velocity criterion, if the two velocity curves are separated, like curve 1 in Fig. 1, it indicates that the crack propagation velocity is less than the decompression wave velocity. And in this case, the crack tip pressure decreases continuously until the crack arrest is realized. If they are tangent to each other (curve 2 in Fig. 1), it just satisfies the requirements of crack arrest. If they intersect (curve 3 in Fig. 1), the pipelines have a higher ductile fracture risk.

The energy criterion indicates that the driving force in the crack propagation process is provided by the energy of the medium in the pipe. Meanwhile, the resistance to crack propagation of the pipe itself exists in this process[9]. When the crack driving force is lower than the resistance, the crack is arrested.

2.2 Crack arrest mechanism of different crack arrestors

Crack arrest can be achieved by using crack arrestors to increase the crack resistance[10]. Based on the measures of pipe crack arrest, including the material aspect and the structure aspect, the crack arrestors can be divided into the overall pipeline reinforcement, coaxial crack arrestor and external crack arrestor. In this study, the pipeline overall reinforcement and coaxial crack arrestor of pipeline were studied.

(1) Pipeline overall reinforcement

Pipeline overall reinforcement that increases the overall pipe wall thickness thus increasing the pipe toughness and the crack resistance is usually considered to be the first defense line to control fracture propagation and realize crack arrest.

(2) Coaxial crack arrestor

The coaxial crack arrestor is generally composed of pipe sections with different mechanical properties or specifications from the main pipe. A common structure is to insert pipe sections with the same toughness as the main pipe but larger wall thickness into the middle of the main pipe at certain intervals, as shown in Fig. 2. In this situation, when expanding to the pipe section, the crack tip encounters larger resistance to arrest crack.

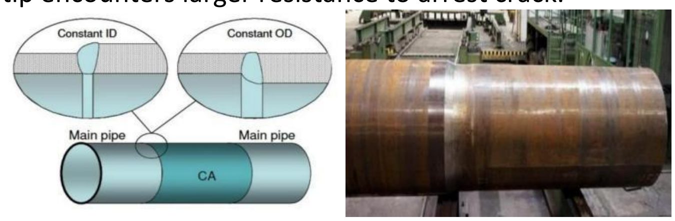

(a)Schematicdiagram (b)Physical map

Fig. 2. Coaxial crack arrestor inserted with larger wall thickness steel pipe

3. PIPELINE OVERALL REINFORCEMENT AND MODELING

3.1 Crack arrest evaluation model of pipeline ductile fracture

At present, some ductile fracture arrest evaluation models have been proposed for different gas pipelines. Among them, standard DNVGL-RP-F104[11] and ISO 27913-2016[12] have put forward corresponding requirements for crack arrest design of CO_2 pipelines. The BTCM is a reliable, accurate and suitable crack arrest evaluation model for CO_2 pipelines, and has been applied to land and submarine pipeline design. Therefore, BTCM was used to study the overall pipeline reinforcement.

The crack propagation velocity and decompression wave velocity can be calculated independently and decoupled[13]. However, due to the particularity of CO_2, the original crack propagation velocity calculation method has errors used to predict the ductile fracture of CO_2 pipeline[14]. For the pipeline material with Charpy V-Notch toughness less than 330 J, the method recommended by ISO 27913-2016 is to use the correction factor $c_{cf} = 1.2$ to correct the relevant hoop stress. In this paper, $c_{cf} = 2$ was adopted to modify the original model of crack propagation velocity calculation.

3.2 Model calculation method

In this section, REFPROP and MATLAB are used to establish the modified BTCM. The calculation flow chart of decompression wave model is shown in Fig. 3. To be noted, the GERG-2008 equation of state in REFPROP software can be used to calculate the sound velocity before the medium enters the two-phase zone. After CO_2 decompression enters the two-phase zone, the physical property parameters in REFPROP database are called by the program with MATLAB language, and the sound velocity is calculated according to the summarized decompression velocity calculation method.

The decompression wave curve and crack propagation curve are established independently, but they are plotted in the same graph. The calculation process of the improved crack propagation velocity curve is shown in Fig. 4. With pressure changes as a reference and an appropriate step size, a complete crack propagation velocity curve can be drawn.

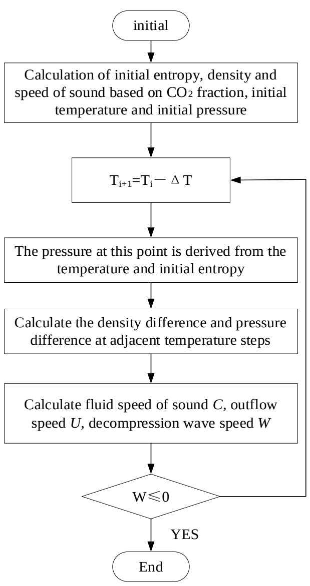

Fig. 3. Flow chart of decompression wave velocity calculation

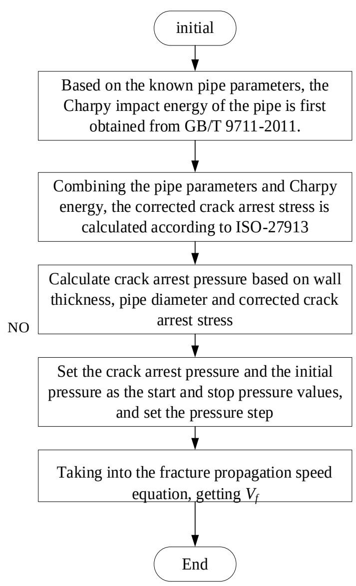

Fig. 4. Flow chart of crack propagation velocity calculation

3.3 *Verification of modified Battelle Two-Curve Model*

According to previous study of our research group[15], the variation trend of decompression wave velocity and pressure platform calculated with GERG-2008 equation of state are consistent with the test values. Fig. 5 shows the the simulation calculation by modified BTCM and test data of the full-scale fracture test of supercritical CO_2 pipeline by Marsili et al[16]. The results show that the modified model of crack propagation velocity is reliable.

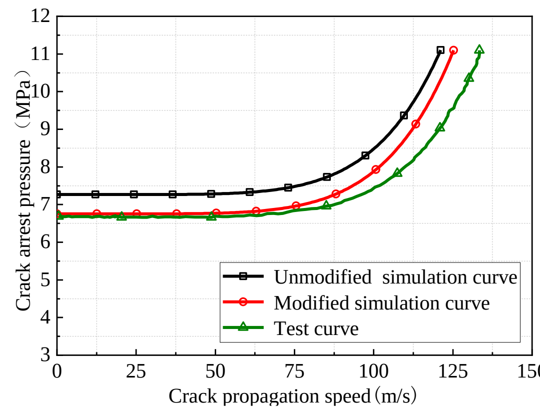

Fig. 5. Variation curves of crack propagation velocity and pressure with different models

4. COAXIAL CRACK ARRESTOR AND MODELING

4.1 *Coaxial crack arrestor and design criteria*

For the supercritical CO_2 pipeline, coaxial crack arrestors were designed to prevent ductile fracture. Its geometric diagram is shown in Fig. 6. Related parameters are defined as follows: *D* is the pipe outer diameter; *t* is the pipe wall thickness; *L* is the coaxial crack arrestor length; *h* is the thickness of coaxial crack arrestor.

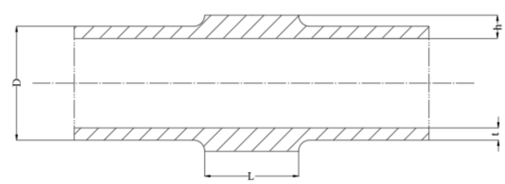

Fig. 6. Geometric diagram of coaxial crack arrestor

4.2 *Coaxial crack arrestor modeling*

For the coaxial crack arrestor, the crack arrest efficiency η is adopted as the criterion of its crack arrest performance. A higher crack arrest efficiency represents a better crack arrest performance of the arrestor. Based on corresponding formulas in Ref.[17], and combined with experimental values of crack arrest efficiency, the MATLAB software was used to fit formula, and the crack arrest efficiency was obtained,

$$\eta = \frac{9.541\left(\frac{E}{\sigma_o}\right)^{0.65}\left(\frac{E}{\sigma_{oa}}\right)^{0.95}\left(\frac{t}{D}\right)^{1.25}\left(\frac{L}{t}\right)^{0.8}\left(\frac{h}{t}\right)^{2.5}}{\left(\frac{P_{CO}}{P_P}-1\right)} \quad (1)$$

in which, E is elastic modulus of the pipeline, MPa; σ_o is the pipeline yield stress, MPa σ_{oa} is the arrestor yield stress, MPa; P_{CO} is the instability fracture pressure of the pipeline; P_P is the propagation pressure, MPa.

4.3 *Verification of coaxial crack arrestor model*

According to the model of crack arrest efficiency, combined with the size parameters of coaxial crack arrestor, the prediction values of crack arrest efficiency were calculated and compared with the test values[18] to verify the model reliability. The test values and prediction values of the crack arrest efficiency are shown in Tab. 1, and the results show that the performance evaluation model based on the crack arrest efficiency of the coaxial crack arrestors is relatively reliable.

5. APPLICATION RESEARCH OF DIFFERENT CRACK ARRESTORS IN YANCHANG OILFIELD UNDER ACTUAL WORKING CONDITIONS

5.1 Analysis of crack arrest for supercritical CO_2 pipeline transportation scheme

Tab. 1 Comparison between test values and prediction values of crack arrest efficiency of coaxial crack arrestor

t (mm)	*h* (mm)	*L*(mm)	η in test	η in prediction	Relative error of η
2.44	5.01	25.32	0.8307	0.8481	2.09%
2.43	4.61	25.31	0.7422	0.7215	-2.78%
2.54	4.38	25.42	0.7242	0.7154	-1.19%
2.58	3.67	25.35	0.4258	0.4125	-3.22%
2.20	3.76	25.40	0.5437	0.5625	3.45%
2.22	4.87	25.42	1.0097	0.9859	-2.41%

The medium in CCUS program of Yanchang Oilfield mainly comes from high-purity CO_2 captured in the coal-to-oil process, with a composition of up to 96%-99% and a few of impurities.

5.1.1 Pipeline parameters

The transportation conditions and pipe parameters of pipelines L21-L25 in this scheme are summarized in Tab. 2.

5.1.2 Evaluation of crack arrest ability

The modified BTCM was adopted to calculate and analyze the decompression wave velocity and the crack propagation velocity curves based on the transportation conditions and pipeline specifications of pipelines L21-L25. According to Appendix G of GB/T 9711-2017[18], the Charpy energy value of X80 steel is 80-180 J.

Tab. 2. Summary of design parameters for pipelines L21-L25

Parameters	L21	L22	L23	L24	L25
Nominal diameter（mm）	DN400	DN400	DN400	DN200	DN250
Pipe grade	X80	X80	X80	X80	X80
Pipe specification（mm）	$\emptyset 406 \times 12$	$\emptyset 406 \times 12$	$\emptyset 406 \times 12$	$\emptyset 219 \times 7$	$\emptyset 273 \times 9$
Flow rate（million t/a）	3.70	3.02	2.83	0.10	0.15
Pipe length（km）	194	33	36	90	110
Pipe buried depth（m）	1.8	1.8	1.8	1.8	1.8
Ground temperature of pipe（℃）	7.8	7.8	7.8	7.8	7.8
Inlet pressure（MPa）	12.50	14.50	14.06	17.30	17.30
Outlet pressure（MPa）	8.381	14.06	13.619	13.976	14.356
Inlet temperature（℃）	45	22.18	17.29	17.31	17.31
Outlet temperature（℃）	14.08	17.29	13.40	7.87	8.11

Fig. 7 shows the curves of the decompression wave/crack propagation velocity and pressure of pipelines L21-L25. As shown in Fig. 7(a), the platform pressure of decompression wave in pipeline L21 is the highest of 7.7MPa, much higher than 5.6MPa in pipeline L22 and 5.2MPa in pipeline L23. When Charpy energy is 80 J, the corresponding crack propagation velocity curve intersects with the decompression wave velocity curve of pipelines L21-L23. Even if Charpy energy increases to 180 J, they also intersect with each other for L21 and L22, and the crack cannot be arrested.

From Fig. 7 (b) and (c), the crack arrest pressure of pipelines L24 and L25 is 5.8 MPa and 5.6 MPa respectively, both higher than the platform pressure of decompression wave. When the Charpy energy of the two pipes is 80 J, the two kinds of velocity curves do not intersect, which represents L24 and L25 can arrest crack.

5.2 Crack arrest scheme for non-crackable pipes

To make the non-crackable pipelines L21-L23 arrest crack, the overall reinforcement method was firstly used. The crack arrest pressure that can be provided by the reinforced pipeline was calculated and analyzed to meet the requirements of crack arrest toughness. The actual pipe wall thickness should be selected based on the calculation results of the minimum pipe wall thickness and further referring to GB/T 17395-2008[19].

5.2.1 Evaluation of pipeline overall reinforcement

As shown in Fig. 8, as the wall thickness of pipelines L21-23 increases to 21.7mm, 15.3mm and 14.2 mm, the crack arrest pressure provided by the pipe is equal to the platform pressure of decompression wave, which just meets the requirements for crack arrest. Referring to GB/T 17395-2008, the wall thickness should be selected as 22mm, 16mm and 15mm, respectively. For these pipes with selected pipe thickness, the minimum crack arrest pressure provided is greater than the relevant platform pressure of decompression, which shows that pipelines L21-L23 can arrest crack using this pipeline overall reinforcement scheme.

5.2.2 Evaluation of coaxial crack arrestor scheme

The results in section 5.2.1 show that the wall thickness of pipeline L21 should increase from 12 mm to

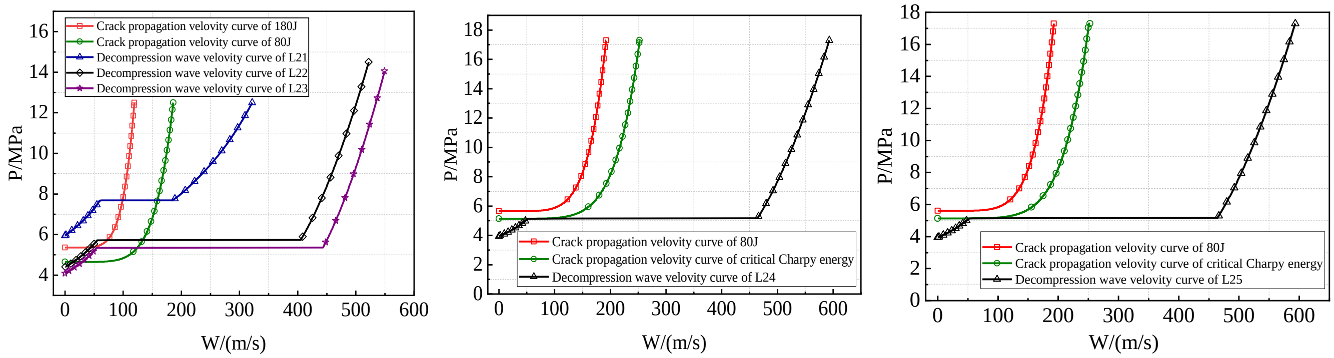

(a) L21-L23 (b) L24 (c) L25

Fig. 7. Decompression wave/crack propagation velocity curves for pipelines L21 to L25

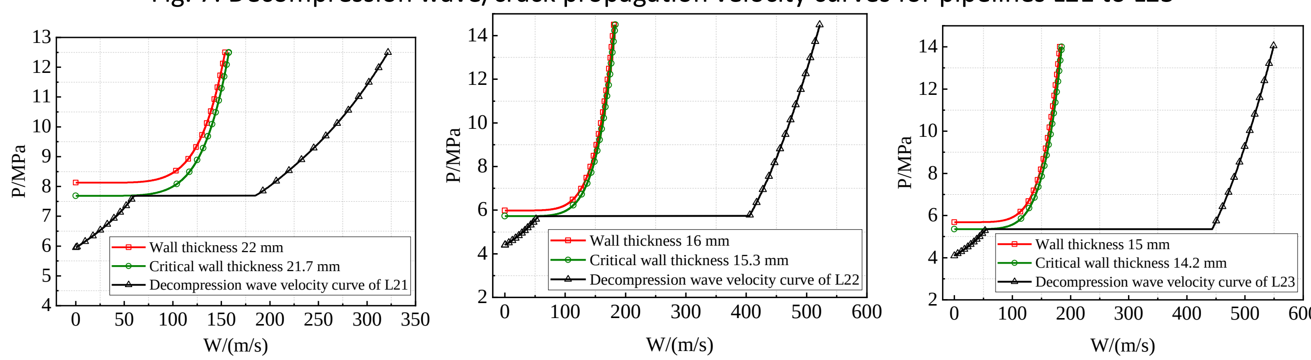

(a) L21 (b) L22 (c) L23

Fig. 8. Decompression wave/crack propagation velocity curves of non-crackable pipelines with increasing wall thickness

22 mm to arrest crack. Obviously, this reinforcement measure is uneconomic, so the coaxial crack arrestor is further considered to reinforce L21.

Based on the performance evaluation model of crack arrest efficiency in section 4.2, the coaxial crack arrestor was designed.. The critical length and thickness of the coaxial crack arrestor that the crack arrest efficiency reaches 1 were calculated, shown in Tab. 3.

The crack arrest ability of pipeline L21 with the coaxial crack arrestor of crack arrest efficiency of 1 was calculated using the modified BTCM. The relevant simulation results are shown in Fig. 9, indicating that it can arrest crack.

Tab. 3. Design parameters of coaxial crack arrestor applied to L21 (when crack arrest efficiency is 1)

Tube	The minimum critical length *L*m/minimum critical thickness *h*cm	The maximum critical length *L*/the maximum critical thickness *h*
X80	*L*m=0.5D(203mm)	*h*=2.55t(30.6mm)
X80	*h*cm=1.64t(19.6mm)	*L*=1.98D(804mm)

6. CONCLUSIONS

(1) A modified BTCM with the correction factor of hoop stress of $c_{cf}=2$ was proposed to evaluate the crack arrest ability. The crack propagation and decompression wave velocity were calculated by using MATLAB program and REFPROP software, and verified to be more consistent with the full-scale burst test of supercritical CO_2 pipeline.

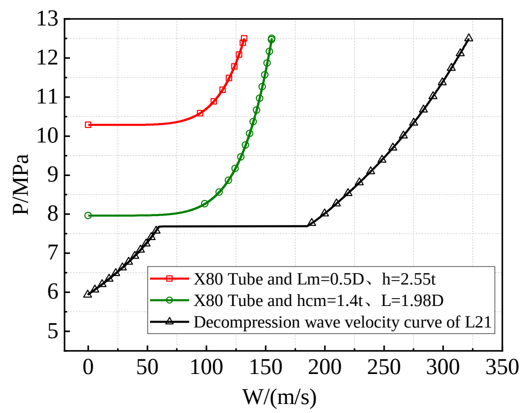

Fig. 9. Decompression wave/crack propagation velocity curves of coaxial crack arrestor applied to pipeline L21 with X80 steel and different size combinations.

(2) For coaxial crack arrestors, a performance evaluation model based on crack arrest efficiency was established, and its reliability was verified by test data.

(3) For five pipelines in CCUS program of Yanchang Oilfield, the modified BTCM was used to evaluate the crack arrest ability. The results show that pipelines L21-L23 cannot arrest crack. For pipes L21-L23, the overall pipeline reinforcement was firstly adopted and evaluated. The wall thickness of L21-L23 increases from 12mm to 22mm, 16mm and 15mm, respectively, to arrest crack.

(4) Since the overall pipeline reinforcement scheme of L21 is uneconomical, the coaxial crack arrestor is considered. For the coaxial crack arrestor with X80 steel whose crack arrest efficiency is 1, the length range is 203 -804 mm and the thickness range is 19.6 -30.6 mm. The coaxial crack arrestor with the crack arrest efficiency of 1 was applied to L21 pipeline, and it can arrest crack.

ACKNOWLEDGEMENT

This research is supported by the National Major Project Yanchang Petroleum Carbon Capture and Flooding Storage Integration Demonstration Project, the Feasibility Study of Liquid CO_2 Pipeline Transportation in Yanchang Oilfield (ycsy2015ky-B-02); and the Shaanxi Provincial Key R&D Program Project, Research on Critical Technologies for the Safety of CO_2 Pipeline Transportation containing Impurities Based on CCUS (2022SF-233).

DECLARATION OF INTEREST STATEMENT

The authors declare that they have no known competing financial interests or personal relationships that could have appeared to influence the work reported in this paper. All authors read and approved the final manuscript.

REFERENCE

[1] Mikhaylov A, Moiseev N, Aleshin K, et al. Global climate change and greenhouse effect. Entrep Sustain Iss 2020; 7(4): 2897.

[2] Ryakhovskikh I V. Model of stress corrosion cracking and practical guidelines for pipelines operation. ENG FAIL Eng Fail Anal 2021; 121: 105134.

[3] Munkejord S T, Austegard A, Deng H, et al. Depressurization of CO_2 in a pipe: High-resolution pressure and temperature data and comparison with model predictions. Energy 2020; 211: 118560.

[4] Hu Q, Zhang N, Li Y, et al. A new model for calculation of arrest toughness in the fracture process of the supercritical CO_2 pipeline. ACS Omega 2021; 6(26): 16804-16815.

[5] Cosham A, Eiber R J, Clark E B. GASDECOM: Carbon dioxide and other components. International Pipeline Conference, American Society of Mechanical Engineers, 2010; 44212: 777-794.

[6] Linton V, Leinum B H, Newton R, et al. CO_2SAFE-ARREST: a full-scale burst test research program for carbon dioxide pipelines—Part 1: project overview and outcomes of test. International Pipeline Conference, American Society of Mechanical Engineers, 2018; 51883: V003T05A008.

[7] Fonzo A, Meleddu A, Di Biagio M, et al. Crack propagation modeling and crack arrestor design for X120. International Pipeline Conference, American Society of Mechanical Engineers, 2006; 42630: 317-325.

[8] Munkejord S T, Hammer M, Løvseth S W. CO_2 transport: data and models – a review. Appl Energ 2016; 169: 499-523.

[9] Goswami S, Anitescu C, Chakraborty S, et al. Transfer learning enhanced physics informed neural network for phase-field modeling of fracture. Theor Appl Fract Mec, 2020; 106: 102447.

[10] Zhuang Z, O'donoghue P E. The recent development of analysis methodology for rapid crack propagation and arrest in gas pipelines. Int J Fracture, 2000; 101: 269-290.

[11] DNVGL-RP-F104.Det Norske Veritas. DNV-RP-F104 Design and operation of carbon dioxide pipelines. Veritasveien, Norway, 2021.

[12] ISO 27913-2016, Carbon dioxide capture, transportation and geological storage — Pipeline transportation systems.

[13] Mohitpour M, Seevam P, Botros K K, et al. Pipeline transportation of carbon dioxide containing impurities. ASME Press, 2012.

[14] Biagio M D, Lucci A, Mecozzi E, et al. Fracture propagation prevention on CO_2 pipelines: full scale

experimental testing and verification approach, Pipeline Technology Conference, Berlin, 2017.
[15] Xu Y. Study on the crack ductility growth of impurity supercritical CO_2 pipeline. Xi'an Shiyou University, 2021.(in Chinese)
[16] Marsili D L, Stevick G R. Reducing the risk of ductile fracture on the canyon reef carriers CO_2 pipeline. SPE Annual Technical Conference and Exhibition, OnePetro, 1990.
[17] Kyriakides S, Lee L. Mechanics of Offshore Pipelines, Volume 2: Buckle propagation and arrest. Gulf Professional Publishing, 2020.
[18] GB/T 9711-2017, Steel pipes for pipeline transportation systems in the oil and gas industry. China: General Administration of Quality Supervision, Inspection and Quarantine of the People's Republic of China, Standardization Administration of China, 2017. (in Chinese)
[19] GB/T 17395-2008, Size, shape, weight and allowable deviation of seamless steel pipes. China: CN-GB, 2008. (in Chinese).